

Optics Letters

High-contrast imaging through scattering media using structured illumination and Fourier filtering

EDOUARD BERROCAL,* SVEN-GÖRAN PETTERSSON, AND ELIAS KRISTENSSON

Division of Combustion Physics, Department of Physics, Lund University, Lund, Sweden

*Corresponding author: edouard.berrocal@forbrf.lth.se

Received 4 October 2016; accepted 3 November 2016; posted 7 November 2016 (Doc. ID 278077); published 1 December 2016

We show in this Letter a novel approach for high-contrast imaging through scattering media by combining structured illumination and Fourier filtering (SIF). To assess the image contrast enhancement at different image spatial frequencies, the modulation transfer function is calculated for four detection schemes: (1) no filtering, (2) Fourier filtering, (3) structured illumination, and (4) SIF filtering. A scattering solution consisting of $D = 7.3 \mu\text{m}$ polystyrene spheres immersed in distilled water and illuminated at $\lambda = 671 \text{ nm}$ is used here. We demonstrate the possibility of obtaining, with SIF, an image contrast up to 60% at an optical depth of $\text{OD} = 10$, improving the contrast by a factor of 40 over conventional transmission imaging. © 2016 Optical Society of America

OCIS codes: (110.4100) Modulation transfer function; (290.4210) Multiple scattering; (110.0113) Imaging through turbid media.

<https://doi.org/10.1364/OL.41.005612>

Visualizing hidden objects within or behind a scattering medium is of importance for a variety of applications such as imaging biomedical samples (e.g., skin tissues) in medicine [1] or spray systems (e.g., diesel and gasoline sprays) in combustion engineering [2]. When light transits through an optically dense turbid medium, most photons participate in multiple scattering interactions. These interactions change photon properties, affecting the optical information that they carry, resulting in the occurrence of blur on the recorded images. By knowing the initial properties of the incident beam, different strategies to filter out the contribution of multiple scattering can be directly implemented in the case of transillumination imaging, as reviewed in [3]. In this source-camera configuration, the detection of unscattered ballistic photon is of interest.

As the initial direction of photon propagation is randomized by the multiple scattering interactions, one filtering strategy consists of preserving the directionality of the collimated incident light. This is done by means of Fourier spatial filtering where a small aperture is used at the center of the focal plane of the imaging lens [4,5]. In addition to directionality, the state of polarization of the incident beam is also affected by multiple scattering events, making a linearly polarized beam randomly polarized. Thus, polarization filtering [6] can also be imple-

mented to reduce the contribution from multiple scattered photons, albeit only by a factor of 2. The approach relies on simply adding a linear polarizer in front of the camera lens, with its orientation corresponding to the incident linear polarization. A third approach, which is able to select the ballistic light, is to exploit coherence. Similar to the directionality and polarization, the coherence of a light beam is lost after multiple scattering interactions. Thus, the ballistic light, which preserves coherence, can be separated from the incoherent scattered light by means of various coherent filtering approaches [3].

Moreover, photons that undergo several scattering processes travel longer paths. Consequently, an ultrashort laser pulse will spread over time while crossing a turbid medium. By time-gating the first photons reaching the collecting lens, the image contrast can be enhanced [7,8]. To significantly improve visibility through turbid media, using this approach requires extremely short gating times, generally on the order of a few picoseconds [2]. In practice, most systems that take advantage of time-gating to mitigate scattered light are based on the use of the optical Kerr effect (OKE) [9]. An OKE shutter consists of the association of crossed polarizers with the birefringent Kerr medium located at its center. Thus, in such an optical scheme polarization filtering is combined with time-gating. In 90 s, the group of Alfano extensively explored the effects of time-gating and Fourier filtering when imaging through turbid media. The authors demonstrated in [4] that spatial Fourier filtering acts as a temporal gate, as photons whose direction of propagation is changed by multiple scattering also have a longer time of flight.

In this Letter, we investigate the potential of using an alternative approach to improve visibility through turbid scattering media. Our approach is based on an illumination technique called structured illumination (SI) [10] in conjunction with spatial Fourier filtering. While SI was first developed in 1997 for obtaining optically sectioned images in microscopy [11], its capability to suppress the multiple light scattering contribution generated in turbid media was only demonstrated a decade later [12,13]. The basic working principle of SI is to take advantage of the fact that image details are sharp only if the light originates from the in-focus plane while, in contrast, photons from the surrounding parts of the sample induce blurring effects. Therefore, by superimposing a spatial modulation (the so-called “structure”) only at the in-focus plane, it becomes possible to differentiate between the in-focus and the out-of-focus

light. Technically, the amplitude of the imaged modulation primarily corresponds to the in-focus light, while the non-modulated component corresponds to multiple light scattering and/or out-of-focus light. Thus, the purpose of SI is to extract the former contribution and to reject the latter. This can be achieved by imaging the superimposed “grid structure” a number of times at different spatial phases. To avoid the formation of residual lines on the final SI image, a minimum acquisition of three modulated images is required, between which the spatial phase of the sinusoidal modulation is shifted by $2\pi/3$. From those three sub-images, denoted I_0 , $I_{2\pi/3}$, and $I_{4\pi/3}$, an image of the intensity amplitude I_f of the sinusoidal modulation of frequency f is extracted without any resolution loss by

$$I_f = \frac{\sqrt{2}}{3} \cdot \sqrt{[I_0 - I_{2\pi/3}]^2 + [I_0 - I_{4\pi/3}]^2 + [I_{2\pi/3} - I_{4\pi/3}]^2}. \quad (1)$$

Note, however, that two mismatched modulated sub-images can also be used to extract I_f with minimal image artifacts if one applies a modulated pattern of sufficiently high spatial frequency [13]. In other situations, where the loss of the image resolution is not a limiting factor, a single modulated sub-image can also be employed [9].

To evaluate the visibility when imaging through a turbid medium, one can use a spatially modulated pattern where the equivalent bright and dark fringes are imaged. For a given modulation frequency, the resulting visibility, known as the Michelson contrast, is defined as

$$M_f = \frac{I_{\max} - I_{\min}}{I_{\max} + I_{\min}} = \frac{I_f}{I_0}, \quad (2)$$

where I_{\max} and I_{\min} correspond to the highest and lowest intensities, respectively.

As mentioned previously, I_f represents the amplitude of the modulation (also named the AC component) and I_0 represent the mean intensity (also named the DC component), as indicated in Fig. 1(a). In the case of a sinusoidal pattern of given modulation frequency f_f , the detected light signal equals

$$I(x) = I_0 + I_f(\sin(2\pi f_f \cdot x)). \quad (3)$$

By taking the complex Fourier transform of $I(x)$, we obtain

$$G(f) = a_0\delta(f) + a_f\delta(f - f_f) + a_{-f}\delta(f + f_f). \quad (4)$$

As $|a_f| = |a_{-f}| = I_f/2$ and $|a_0| = I_0$, the Michelson contrast can then be deduced from Eq. (2) as

$$M_f = \frac{I_f}{I_0} = \left| \frac{2a_f}{a_0} \right|. \quad (5)$$

Now in the case of a square pattern of modulation frequency f_f , the Fourier spectrum is

$$G(f) = \frac{a_0}{2}\delta(f) + \frac{a_f}{\pi}\delta(f - f_f) + \frac{a_{-f}}{\pi}\delta(f + f_f) + H.F., \quad (6)$$

where *H.F.* corresponds to higher frequency components. In this case, the resulting Michelson contrast is deduced as

$$M_f = \left| \frac{\pi a_f}{2a_0} \right|. \quad (7)$$

The modulation transfer function (*MTF*) is commonly used in imaging to assess the performance of an optical system, and

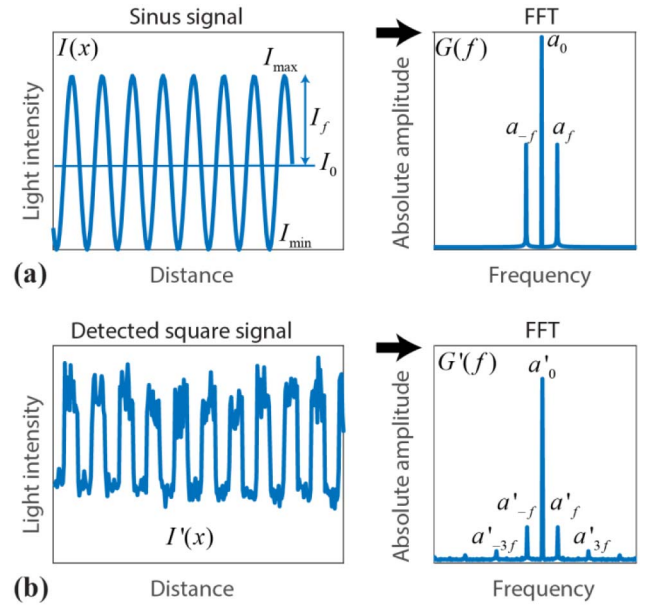


Fig. 1. For a theoretical sinusoidal signal, shown in (a), the fundamental frequency has half the amplitude of the zero-order frequency. In the case of a square pattern recorded experimentally, shown in (b), the Fourier spectrum now has more frequencies, and the amplitude of the fundamental is reduced while background noise is present.

corresponds to the ratio between an output modulation and the input modulation of a sinusoidal pattern, such as

$$MTF_f = M'_f/M_f. \quad (8)$$

In the case of a perfect square pattern at the input where $M_f = 1$, the *MTF* can be directly deduced from the calculation of the image contrast M'_f observed after transmission of the square pattern through the scattering medium. In this case, by using the amplitude of the fundamental frequency a'_f and the amplitude of the zero component, it is deduced that $MTF_f = |\pi a'_f/2a'_0|$.

Note that the effects of a turbid medium on the *MTF* of an optical system have been originally investigated, both numerically and experimentally by the group of Zaccanti and co-workers [14,15]. The authors could find a good agreement between the experimental and numerical data, validating their Monte Carlo code for the simulation of image propagation through random media. In addition, the use of sector star patterns to extract the *MTF* from a single image has been presented elsewhere [16].

The experimental setup used in this Letter is depicted in Fig. 2 and consists of a CW laser beam ($\lambda = 671$ nm) illuminating a sinusoidal grating of 5 lp/mm. The sinusoidal pattern is displaced by translating the grating along the modulation direction to generate the three sub-images I_0 , $I_{2\pi/3}$, and $I_{4\pi/3}$ used to apply SI [see Eq. (1)]. The structured beam illuminates a sector star target of 10 mm diameter containing 36 black sectors. After crossing a water suspension of scattering microspheres of 7.3 μm in diameter, the optical signal is filtered prior to image formation by inserting an aperture in the Fourier plane of the objective lens. The aperture is set to 2.6 mm which helps in the suppression of multiple light scattering while keeping most of the spatial

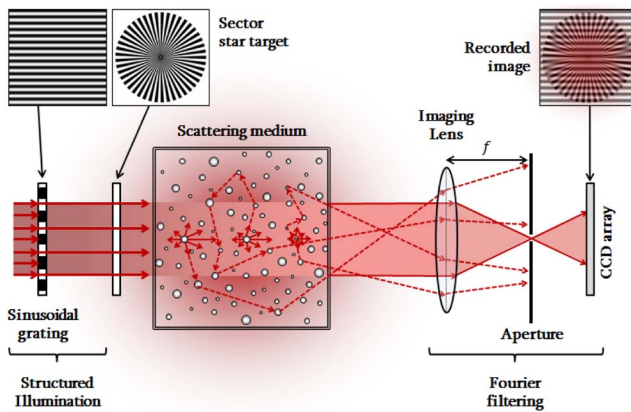


Fig. 2. Experimental setup: a structured laser beam of 5 lp/mm frequency is created using a sinusoidal grating. The beam illuminates a sector star target which is imaged after crossing a scattering suspension of microspheres. The sinusoidal pattern is displaced to generate the sub-images I_0 , $I_{2\pi/3}$, and $I_{4\pi/3}$ by translating the grating between exposures. Finally, the optical signal is also filtered in the Fourier plane of the imaging lens, prior to image formation.

frequency components. The target is then imaged onto a CCD array (Andor, LucaR with 1002×1004 pixels). The exposure time is set to 1 ms, and an averaged image over 10 exposures is deduced. For each averaged image, a corresponding background image is recorded and subtracted.

The light intensity along a circle of radius r from the star center, as indicated in the top right image from Fig. 3, is extracted to generate a one-dimensional square signal similar to the one shown in Fig. 1(b).

The resulting curve is then Fourier transformed to determine a'_f and a'_0 which are used to deduce the MTF. This is operated at each radius, and a curve of the MTF as a function of the spatial frequency is extracted for various detection conditions. The high-frequency components are obtained for small r , while the low spatial frequencies are obtained at large r . The fundamental spatial frequency at a certain radius r is given by $f_r = 36/2\pi r$. As the radius of the sector star is 5 mm, the minimum measured spatial frequency then equals 1.15 line-pairs/mm. The sampling limit—the highest spatial frequency observable—is defined by the Nyquist frequency. As the presented images have a pixel resolution of $\sim 10 \mu\text{m}$, this corresponds to a Nyquist frequency of 50 line-pairs/mm.

Figure 4 shows the resulting MTF as a function of the spatial frequency for various detection schemes and optical depths. The optical depth is defined as

$$\text{OD} = N \cdot \sigma_e \cdot L. \quad (9)$$

In the current experiment, the number density of scattering microspheres is $N \sim 2.910^6$ particles/ml, the extinction cross section is calculated from the Lorenz–Mie theory resulting in $\sigma_e = 8.610^{-5} \text{ mm}^2$, and the length crossed by the beam is either $L = 30$ or $L = 40$ mm corresponding to an optical depth of ~ 7.5 or ~ 10 , respectively.

In Fig. 4(a), no scattering particles are added in the cuvette. In this case, the optical depth equals zero and the MTF leads to a contrast near to 100% at low spatial frequencies. The reduction of the MTF with an increase in frequency is induced by the

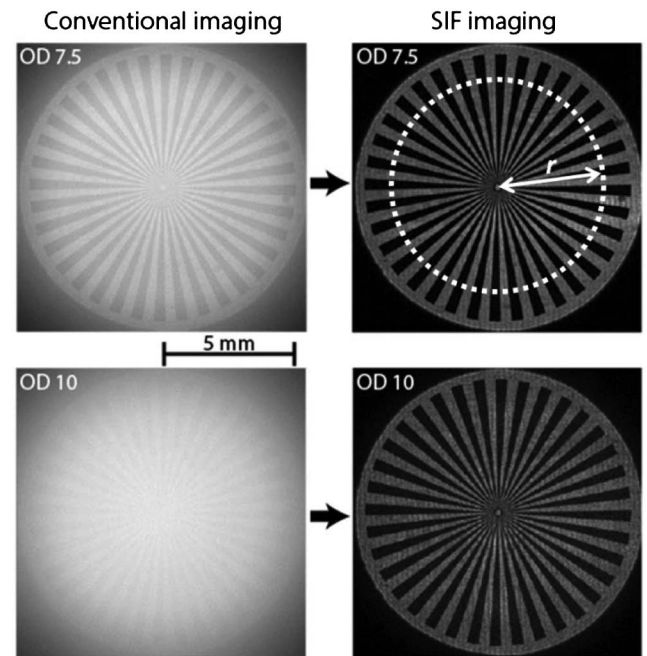


Fig. 3. Sector star target is imaged through a water suspension cuvette containing $7.3 \mu\text{m}$ polystyrene microspheres with optical depths of $\text{OD} = 7.5$ and $\text{OD} = 10$. As shown in the left images, imaging without any filtering strategy, leads to poor visibility of the target. In contrast, when structured illumination and Fourier filtering are combined, the resultant image is clearly visible. The visibility improvement of those images is quantified from their MTFs.

reflection effects through the water cell and the quality of the imaging optics. Even in this situation, without scattering particles, the overall contrast obtained with no filtering can be improved by using structured illumination or Fourier filtering. In the case of Fourier filtering, a clear cut is visible at 30 lp/mm corresponding to the 2.6 mm aperture inserted at the Fourier plane of the camera objective. Note that for a computer-generated perfect black and white sector star pattern, where the MTF should be equal to 1 at all frequencies, a reduction of the contrast with some fluctuations is observed at high frequencies, as shown by the black curve. This is due to the sampling effects at high frequencies which affects the contrast calculation in the Fourier domain.

In Fig. 4(b), the microsphere particles are added in a cuvette of $L = 30$ mm, producing an optical depth of 7.5. Without applying any filtering strategies, the maximum calculated contrast is reduced by a factor of 18, down to $\sim 5\%$. By applying Fourier filtering, the image contrast increases to nearly 30% while the corresponding value for SI is 67%. By combining these two filtering approaches, a contrast above 90% is obtained with SIF, reaching the contrast values obtained previously without any scattering particles.

In Fig. 4(c), a cuvette of $L = 40$ mm is now used with the exact same suspension, resulting in an optical depth of 10. At this high opacity, the image contrast is further reduced below $\sim 1, 5\%$ for the conventional (non-filtered) case, making the star pattern almost entirely concealed due to scattering. The MTF is increased to nearly 7% by applying Fourier filtering and boosted to 20% with SI. Combining Fourier

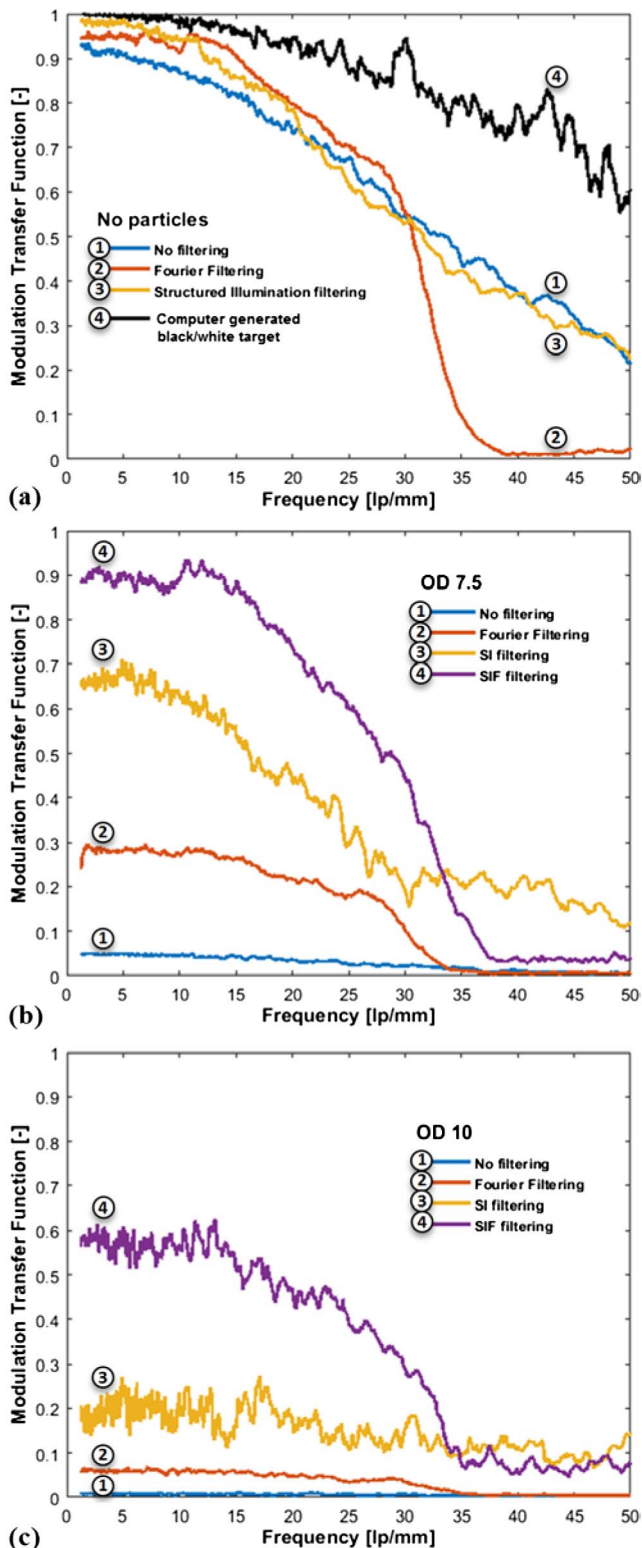


Fig. 4. MTF curves as a function of spatial frequency: in (a), the cuvette is filled with clear water only showing a high contrast for each detection scheme. The MTF for a perfect black and white target is added to show the sampling effects on the MTF at high frequencies. In (b) and (c), the contrast is now reduced due to the presence of scattering microspheres at optical depths of 7.5 and 10, respectively. It is observed that SIF filtering is capable of providing back a high-image contrast equal to 0.9 and 0.6 at OD = 7.5 and OD = 10, respectively.

filtering and SI leads to a clear improvement in visibility and image contrast, with a maximum of 60%, i.e., a boost by a factor of 40 compared to conventional transmission imaging.

Based on these observations and calculations, it can be concluded that spatial Fourier filtering and structured illumination have different filtering capabilities which are complementary and, when the methods are combined, they render an image contrast that greatly exceeds the sum of the two. This can be explained as Fourier filtering rejects a large portion of photons which have been scattered multiple times, making the previously non-visible SI pattern visible again. With the spatially modulated illumination being visible, SI can then be applied to suppress the remaining light intensities from multiple scattered photons. This image improvement comes, however, at the cost of losing some high spatial frequencies and reducing light intensity. Therefore, there is a trade-off between the blocking of multiple light scattering and the preservation of the image information when operating the Fourier filtering. In our case, the 2.6 mm aperture corresponds to a cutoff frequency of 30 lp/mm, preserving most of image information.

Due to its simplicity and high performance, the presented technique could be suitable for a large number of applications related to light transmission through turbid media. While the capability of the technique was demonstrated based on averaged imaging with three modulated sub-images, the possibility of instantaneous imaging of rapidly moving samples, e.g., atomizing sprays, could be achieved using a two-phase structured illumination approach [17].

Funding. European Research Council (ERC) (638546).

REFERENCES

- V. V. Tuchin, *Handbook of Photonics for Biomedical Science* (CRC Press, 2010).
- M. Linne, *Prog. Energy Combust. Sci.* **39**, 403 (2013).
- C. Dunsby and P. M. W. French, *J. Phys. D* **36**, R207 (2003).
- Q. Z. Wang, X. Liang, L. Wang, P. P. Ho, and R. R. Alfano, *Opt. Lett.* **20**, 1498 (1995).
- H. Ramachandran and A. Narayanan, *Opt. Commun.* **154**, 255 (1998).
- S. Mujumdar and H. Ramachandran, *Opt. Commun.* **241**, 1 (2004).
- L. Wang, P. P. Ho, X. Liang, H. Dai, and R. R. Alfano, *Opt. Lett.* **18**, 241 (1993).
- D. Sedarsky, E. Berrocal, and M. Linne, *Opt. Express* **19**, 1866 (2011).
- K. Sala and M. C. Richardson, *Phys. Rev. A* **12**, 1036 (1975).
- E. Berrocal, J. Johnsson, E. Kristensson, and M. Aldén, *J. Eur. Opt. Soc.* **7**, 12015 (2012).
- M. A. A. Neil, R. Juškaitis, and T. Wilson, *Opt. Lett.* **22**, 1905 (1997).
- E. Berrocal, E. Kristensson, M. Richter, M. Linne, and M. Aldén, *Opt. Express* **16**, 17870 (2008).
- E. Kristensson, E. Berrocal, M. Richter, S. G. Pettersson, and M. Aldén, *Opt. Lett.* **33**, 2752 (2008).
- P. Brusciaglioni, P. Donelli, A. Ismaelli, and G. Zaccanti, *J. Mod. Opt.* **38**, 129 (1991).
- P. Donelli, P. Brusciaglioni, A. Ismaelli, and G. Zaccanti, *J. Mod. Opt.* **38**, 2189 (1991).
- E. Marom, B. Milgrom, and N. Konforti, *Appl. Opt.* **49**, 6749 (2010).
- E. Kristensson, E. Berrocal, and M. Aldén, *Opt. Lett.* **39**, 2584 (2014).